A NEW TECHNIQUE TO OBTAIN THE REAL CAPILLARY PRESSURE-SATURATION CURVE DIRECTLY FROM CENTRIFUGE EXPERIMENTS

Giovanna Ragazzini, Carlo Venturini
Agip SpA, S. Donato Milanese MILANO, ITALY

Abstract Determination of the true capillary pressure vs. saturation curve by the centrifuge method has been and still is object of several studies. This problem was first solved with mathematical algorithms whose solutions are derived using some assumptions and approximations which are not always correct. The new approach, described in this paper, enables the analyst to obtain hard saturation data directly from centrifuge experiments. The advantage of this technique is that saturation data have not to be corrected by complex mathematical equations. The new idea is to avoid having an average saturation, which is affected by the end effect in the sample. The far end of the centrifuged sample is equipped with a porous end-piece whose capillary contact with the rock sample is ensured by a layer of cellulose fibre. The whole assembly is then treated as a unique sample undergoing the very same activities as standard samples. The validation of this technique is demonstrated by the comparison of the capillary pressure curve of samples in capillary contact with the end-piece with that obtained through the application of the most recent mathematical formulae. This technique is supported also by comparison with the experimental capillary pressure curve of the inlet piece obtained subdividing the samples in several pieces.

Some experimental results of oil-brine and air-brine

drainage on Sandstone samples having different permeabilities are presented together with an analytical discussion of the results.

INTRODUCTION

The saturation - capillary pressure curve (the pressure difference between the non-wetting and the wetting fluids), that is the relationship between fluid saturation at any point in a porous rock and the corresponding capillary pressure, is a very important correlation for the determination of the initial fluids saturation distribution (gas, oil and brine) in a reservoir.

Among the different laboratory techniques (Omoregie, 1988), the centrifuge method is one of the most used being rapid and as accurate as the other methods.

In centrifuge experiments a problem of data interpretation arises because, once equilibrium is reached at each fixed speed, the average and not the local fluids saturation in the core is measured.

In a spinning sample, in fact, at each constant speed, fluid saturation is not constant, but varies along the sample length due to the presence of a pressure gradient induced by the artificial gravitational field resulting from the rotation and varying with the radius.

Focusing on drainage experiments, assuming the boundary condition $P_c=0$ at $r=R_2$, from the equation of hydrostatic equilibrium in each phase, at each location along the sample, the capillary pressure value is calculated using the following equation:

$$P_c(r) = \frac{1}{2} \Delta\varrho \, w^2 \, (R_2^2 - r^2) \quad (1)$$

The capillary pressure at the inner radius of rotation of the sample is obtained replacing r by R_1. So, at each fixed speed, $P_c(r) \le P_c(R_1)$ for $R_1 \le r \le R_2$.

For example, in the case of an air-brine drainage the capillary pressure trend along the sample length is plotted in Figure 1

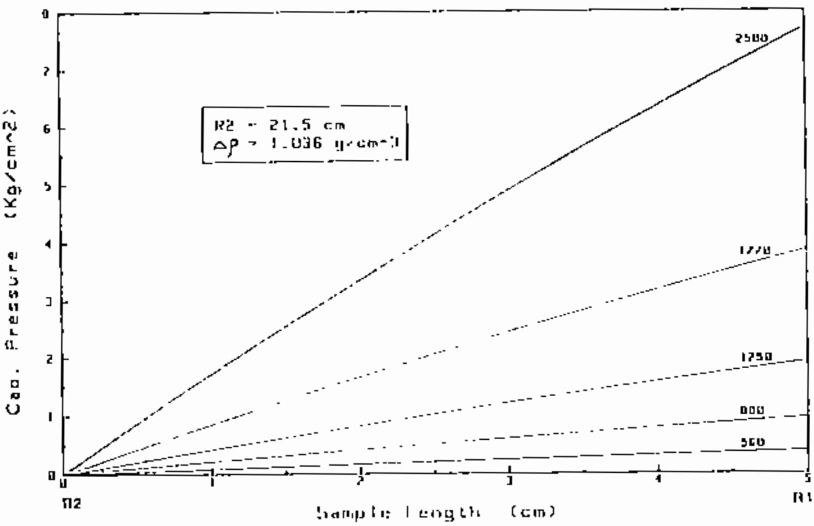

FIGURE 1 Capillary pressure variation in the sample.

for some of the centrifuge rotational speeds used in this study.

Brine saturation has a low value at the inlet face (near to the rotation axis) where capillary pressure is maximum and is 100% at the outlet face (the other end of the sample) where capillary pressure is zero.

The most used procedure to obtain capillary pressure curve from centrifuge experiments is to correct the brine displaced from the sample by means of one of the formulae presented in the Appendix.

THE NEW TECHNIQUE

Due to the difficulty in interpreting and deriving mathematically the average saturation data (see Appendix), a new technique is presented here to obtain saturation data directly from centrifuge experiments, without using a purely analytical approach.

The new method permits the analyst to avoid measuring the saturation in that part of the sample which is affected by the end effect and, consequently, which has the highest saturation. For this purpose a porous end-piece is placed at the outlet end of the examined sample.

This end-piece - taken close to the sample in the core and characterized by the same lithology and permeability as the core sample - has to be in capillary contact with the sample in order to simulate the displacement in a longer sample.

At each speed, once fluids equilibrium is reached, the core saturation is determined by weighing only the core sample. Such saturation values are significantly lower (especially for the lowest capillary pressure values) than those obtained centrifuging the core sample without the end-piece.

The capillary pressure curve is obtained using the sample average saturation vs. the average capillary pressure of the whole system (sample plus end-piece) for each rotational speed.

Drainage displacements (air-brine and oil-brine) are conducted on Sandstone samples of different permeabilities (the usual ones that may be found in reservoirs) in order to check the validity of the proposed method on all trends of capillary pressure curves.

The radial brine saturation distribution is obtained from the drainage in samples subdivided in five pieces each 1 cm long.

In particular the inlet piece capillary pressure curve is very important because it can be considered the "true" capillary pressure curve.

Then the inlet piece curve is compared to the trends calculated using Rajan's and Forbes' solutions applied to the average experimental saturation data of samples (having the same petrophysical properties of the samples subdivided in pieces).

Drainage results of the samples in capillary contact with their end-pieces are compared with the previous curves in order to choose the best end-piece length.

The validation of this technique is supported by comparing the capillary pressure curve obtained using this method with:

1. the curves derived from the application of the most recent (and more accurate) mathematical formulae (Rajan's and Forbes' solutions);
2. the inlet piece capillary pressure curve.

Figure 2 is a diagram of the experimental and interpretative parts of this study.

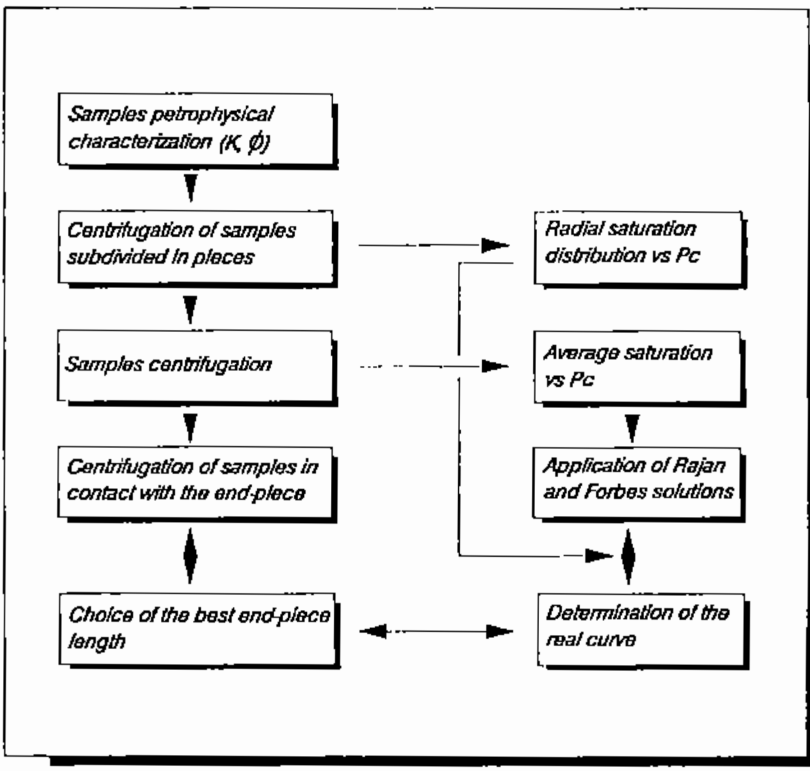

FIGURE 2 Scheme of the study.

EXPERIMENTAL

Apparatus

A standard Beckman J6M refrigerated centrifuge, modified in order to permit both the use of International 287 Oil Test Rotor (four places swinging buckets) and the reading of the liquid displaced from the plugs, is used for this study at various speeds up to 3500 rpm.

Two types of buckets are used: a series made in plexiglass with a graduated end part (Figure 3A) and a series in aluminium which allows one to have the maximum rotational radius (Figure 3B).

A perforated separator is placed at the bottom of the latter to prevent the displaced fluid from imbibing into the sample during centrifuge deceleration.

Capillary contact between samples and end-piece is ensured by use of small disks of Kleenex paper saturated with brine.

Sample Preparation

The core samples here studied were taken from homogeneous Sandstone cores recovered from an oil well and from a Berea Sandstone outcrop.

The samples, approximately 5 cm long and 2.7 cm in diameter, were selected covering different permeability values (30-760 mD). Other samples with the same petrophysical properties were marked (with letters and a line along their length) before being cut in five pieces (1 cm long each) in order to ensure that they were always centrifuged in the same order and position (see Figure 4).

Standard Soxlet extraction, using alternating chloroform and methyl alcohol/water mixture, was applied until the effluent became clear in order to clean all the samples studied.

Drying was then carried out in an oven at 100°C.

Permeability measurements were performed by the steady-state method using nitrogen at three different pressures in order to apply the Klinkenberg correction.

Porosities were determined by the water resaturation method (see Table 1).

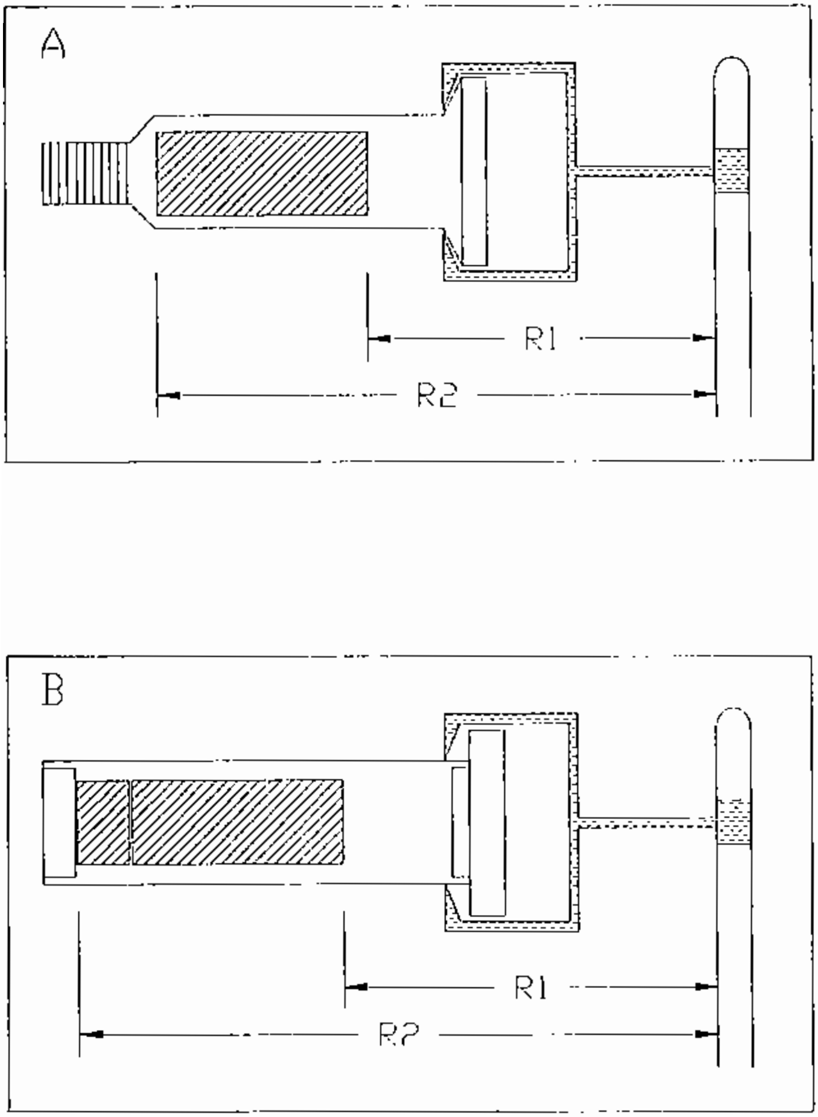

FIGURE 3 Experimental apparatus: A) plexiglass bucket, B) aluminium bucket.

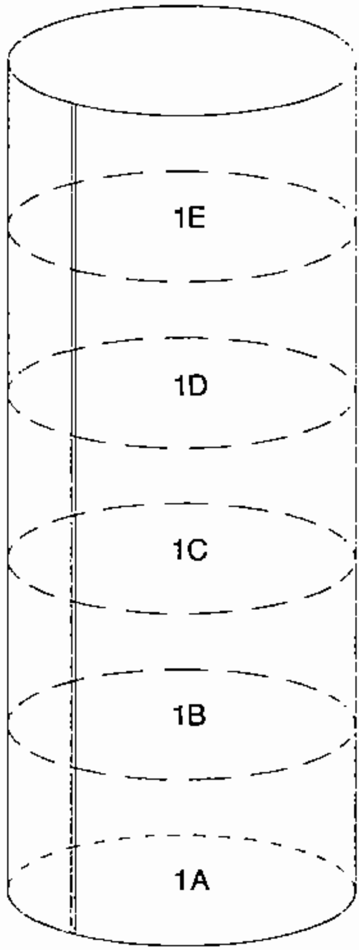

FIGURE 4 Sliced sample.

TABLE 1 Petrophysical properties of the samples.

Sample (n°)	L (cm)	D (cm)	K (mD)	Ø (%)
1	4.9	2.7	192	18.6
2	4.9	2.7	757	21.3
3	4.9	2.7	31.7	16.8
4	4.9	2.7	85.8	15.0

To ensure complete water saturation, all the samples were placed in a cell, vacuum applied for half an hour and then killed by CO_2. This operation was repeated twice and then high vacuum at 0.1 μm Hg was applied for 8 hours. The cell was then filled with brine (filtered at 0.45 μm) and the pressure was increased and maintained overnight at 15 MPa.

This procedure was repeated at the end of each drainage, petrophysical measurements of all the core samples studied were determined each time before beginning a new drainage in order to check possible variations of their properties.

Test Procedure

Samples were then submitted to a series of centrifuge tests as follows:

1. Two air-brine drainage tests were performed on the whole samples using the two methods of calculating saturation: i) stopping centrifuge (for 20 min) and weighing the samples (using aluminium bucket); ii) reading the volume of the fluid displaced during centrifugation (using plexiglass bucket); to check whether or not the first method affects saturation equilibria.
2. Radial brine saturation distribution was obtained from tests performed on the five pieces. The capillary contact between them was ensured by use of Kleenex disks (Kimberly-Clark, code

6056). Saturation was determined by weighing each piece after a minimum rotation time of eight hours for each speed.

3. Capillary pressure curve vs. average brine saturation was obtained on the whole samples without the end-piece in order to calculate the capillary curves corrected using equations (A3) and (A4).

4. The same samples were then tested with the new method using an end-piece at their outlet end. For each rotational speed, the average brine saturation was measured by weighing the whole samples without their end-pieces and the capillary pressure considered was the average of the whole system.

The experimental conditions for these drainage tests are shown in Table 2.

EXPERIMENTAL RESULTS

The experimental results from air-brine drainage performed using plexiglass buckets and reading directly the volume of brine displaced by means of a stroboscope lamp without stopping centrifuge are presented in Table 3.

The experimental results of both the air-brine and oil-brine drainage tests including rotational speeds, the capillary pressure

TABLE 2 Drainage experimental conditions.

EXPERIMENTAL CONDITIONS	
Brine salinity (as NaCl)	50,000 ppm
Brine density	1.036 g/cm^3
Oil density	0.756 g/cm^3
Temperature	21° C
Equilibrium time (minimum)	8 h
Rotation radius (R_2):	
plexiglass bucket	12.8 cm
aluminium bucket	21.5 cm

TABLE 3 Saturation data obtained without stopping centrifuge.

Pc (kg/cm2)	BRINE SATURATION (%)			
	SAMPLE 1	SAMPLE 2	SAMPLE 3	SAMPLE 4
0.13	98.3	82	100	99.2
0.36	67.7	45.4	90.2	75.8
0.9	42.9	30.6	58.9	46.8
1.79	31.6	23	43.7	34.6
3.56	25.8	16.9	33.3	27.1

values and the saturations (experimental and calculated) of the whole samples and of the small pieces are shown in Tables 4-6.

The saturation results, obtained placing the end-piece at the bottom of the whole samples, are shown in Table 7.

Discussion

Comparing the results in Table 3 with those in Tables 4-5 ("Avg" column), no big difference in brine saturation is detected from tests performed by stopping or not stopping the centrifuge during the test.

For all the drainage tests the average saturation calculated from the saturation profile (see Tables 4-6) corresponds (in the experimental error range) to the average saturation of the whole samples measured experimentally. This is another proof (besides permeability and porosity values) of the homogeneity of the small pieces compared to the equivalent whole samples. So, it can be stated that the saturation profile obtained from the sliced samples (see Tables 4-6 and Figure 5) is the same as that of the corresponding whole samples.

Capillary pressure curve of the inlet piece can be considered the almost true trend because in this piece the capillary pressure gradient is always lower than in the other pieces. It is negligible for the lowest speeds, while on increasing rotational speed

TABLE 4 Air-brine drainage experimental and calculated data of the most permeable samples.

	CAPILLARY PRESSURE			BRINE SATURATION (%)					
				SAMPLE 1			SAMPLE 2		
RPM	Inlet	Inlet/2	Forbes	Avg	Rajan	Forbes	Avg	Rajan	Forbes
330	0.13	0.065		98.2	82.7		80.2	43.8	
400	0.19	0.095	0.17	92.8	53.1	82	62.5	36.3	27.2
560	0.38	0.19	0.3	69.4	38.5	48.1	43.4	26.2	26
880	0.93	0.465	0.71	41.8	26.3	24.6	29	18.1	20
1250	1.88	0.94	1.5	32	20.2	23.3	21.4	14	14.6
1770	3.77	1.885	3.01	24.4	16.1	17.5	18.6	11.4	14.2
2500	7.51	3.755	6.01	18.8	13.3	13.7	13.2	9.6	9.2
3500	14.73	7.365	11.84	14.3	11.4	10	10.3	8.5	7.6

RPM	PIECE 1A		PIECE 1B		PIECE 1C		PIECE 1D		PIECE 1E		
	Pc	Sw	Pc	Sw	Pc	Sw	Pc	Sw	Pc	Sw	Avg Sw
330	0.01	100	0.04	100	0.07	99.9	0.1	99.1	0.12	91.8	98.16
400	0.02	99.2	0.06	98.8	0.11	96.4	0.14	95.4	0.18	69.7	91.9
560	0.04	97.3	0.13	82.6	0.21	64	0.28	54.1	0.35	41.3	67.86
880	0.11	71.5	0.31	47	0.51	36.1	0.69	31.5	0.87	28.1	42.84
1250	0.21	58.1	0.63	34.2	1.02	27.9	1.4	25.1	1.75	20.1	33.08
1770	0.43	41.4	1.26	25.3	2.05	21.9	2.8	19.6	3.51	17.4	25.12
2500	0.85	34.8	2.51	20.8	4.09	17.7	5.59	15.1	7	12.9	20.26
3500	1.67	26.5	4.92	14.8	8.02	13.2	10.95	11.5	13.73	10	15.2

RPM	PIECE 2A		PIECE 2B		PIECE 2C		PIECE 2D		PIECE 2E		
	Pc	Sw	Pc	Sw	Pc	Sw	Pc	Sw	Pc	Sw	Avg Sw
330	0.01	99.3	0.04	97	0.07	87.4	0.1	59.3	0.12	46.9	77.98
400	0.02	92.1	0.06	82.9	0.11	50	0.14	41.9	0.18	34.9	60.36
560	0.04	70.9	0.13	55	0.21	35.6	0.28	31.7	0.35	27.8	44.2
880	0.11	42.8	0.31	28.9	0.51	24.2	0.69	22.1	0.87	20.1	27.62
1250	0.21	31.3	0.63	22.6	1.02	19.1	1.4	17.4	1.75	16	21.28
1770	0.43	25.9	1.26	17.4	2.05	15.7	2.8	14.1	3.51	12.8	17.18
2500	0.85	19	2.51	13.6	4.09	12.6	5.59	11.4	7	10.2	13.36
3500	1.67	14.3	4.92	10.5	8.02	9.7	10.95	8.4	13.73	7.6	10.1

TABLE 5 Air-brine drainage experimental and calculated data of the least permeable samples.

	CAPILLARY PRESSURE			BRINE SATURATION (%)					
				SAMPLE 3			SAMPLE 4		
RPM	Inlet	Inlet/2	Forbes	Avg	Rajan	Forbes	Avg	Rajan	Forbes
400	0.19	0.095		99.4	96.2		95.8	55.8	
560	0.38	0.19	0.3	90.6	56.5	82.6	75.2	41.2	48.7
880	0.93	0.465	0.71	60.8	38	42.2	45.2	28.9	29.6
1250	1.88	0.94	1.5	43	28	27.2	35.7	22.7	27.2
1770	3.77	1.885	3.01	32.1	20.9	22.2	27.7	18.4	20.5
2500	7.51	3.755	6.01	23.4	15.7	15.4	20.7	15.5	14.3
3500	14.73	7.365	11.84	17.6	12.1	12.1	14.8	13.5	12.7

	PIECE 3A		PIECE 3B		PIECE 3C		PIECE 3D		PIECE 3E		
RPM	Pc	Sw	Pc	Sw	Pc	Sw	Pc	Sw	Pc	Sw	Avg Sw
400	0.02	100	0.06	98.8	0.11	98.5	0.14	98.4	0.18	98.3	98.8
560	0.04	98.9	0.13	97.8	0.21	95.9	0.28	83.7	0.35	69.6	89.18
880	0.11	89.6	0.31	72.2	0.51	50.7	0.69	44.2	0.87	41.8	59.7
1250	0.21	68.2	0.63	51	1.02	36.8	1.4	34.3	1.75	29.7	44
1770	0.43	49.4	1.26	39.1	2.05	29.5	2.8	26.2	3.51	22.7	33.38
2500	0.85	40	2.51	27.5	4.09	20.8	5.59	18.5	7	16.4	24.64
3500	1.67	32.4	4.92	19	8.02	16	10.95	14.2	13.73	13.1	18.94

	PIECE 4A		PIECE 4B		PIECE 4C		PIECE 4D		PIECE 4E		
RPM	Pc	Sw	Pc	Sw	Pc	Sw	Pc	Sw	Pc	Sw	Avg Sw
400	0.02	99.9	0.06	98.6	0.11	97.7	0.14	93.8	0.18	86.9	95.38
560	0.04	97.7	0.13	94.6	0.21	86.8	0.28	68.3	0.35	44.8	78.44
880	0.11	68	0.31	50.9	0.51	44.1	0.69	39.3	0.87	31	46.66
1250	0.21	50.8	0.63	41.4	1.02	34.5	1.4	31.1	1.75	25.9	36.74
1770	0.43	37.3	1.26	31.6	2.05	27.7	2.8	25.5	3.51	20.2	28.46
2500	0.85	34.5	2.51	25.1	4.09	20.6	5.59	18.4	7	16.5	23.02
3500	1.67	29.1	4.92	18.8	8.02	15.8	10.95	13.8	13.73	13	18.1

TABLE 6 Oil-brine drainage experimental and calculated data of the most permeable samples.

	CAPILLARY PRESSURE			BRINE SATURATION (%)					
				SAMPLE 1			SAMPLE 2		
RPM	Inlet	Inlet/2	Forbes	Avg	Rajan	Forbes	Avg	Rajan	Forbes
530	0.09	0.045		97.1	78		77.5	35.66	
630	0.13	0.065	0.11	87.7	54.1	68.4	62.6	29.55	31.7
760	0.19	0.095	0.17	77.7	46.4	57.7	52.1	24.79	31.1
1070	0.37	0.185	0.3	55.5	35.7	34.2	37.8	19.05	24.1
1690	0.94	0.47	0.7	35.5	25.4	23.8	23.1	14.59	14.5
2400	1.89	0.945	1.5	28.3	20.1	21.8	17.7	12.77	12.8
3500	4.01	2.005	3.1	21	16	15.1	13.5	11.62	10.1

	PIECE 1A		PIECE 1B		PIECE 1C		PIECE 1D		PIECE 1E		
RPM	Pc	Sw	Pc	Sw	Pc	Sw	Pc	Sw	Pc	Sw	Avg Sw
530	0.01	99.6	0.03	99.3	0.05	98.3	0.07	93.3	0.084	90.5	96.2
630	0.014	98.1	0.04	97.7	0.07	91.3	0.09	88.2	0.12	68.2	88.7
760	0.02	97.5	0.06	96	0.1	73.7	0.14	69.9	0.17	50.2	77.46
1070	0.04	90.2	0.12	61.9	0.2	42.4	0.27	37	0.34	35	53.3
1690	0.1	66.8	0.31	38.9	0.5	28.5	0.68	24.1	0.86	23.8	36.42
2400	0.21	49.9	0.62	29.5	1	23.1	1.38	22	1.73	21.1	29.12
3500	0.45	35.3	1.32	22.2	2.15	18.1	2.94	16.9	3.68	16.5	21.8

	PIECE 2A		PIECE 2B		PIECE 2C		PIECE 2D		PIECE 2E		
RPM	Pc	Sw	Pc	Sw	Pc	Sw	Pc	Sw	Pc	Sw	Avg Sw
530	0.01	94.5	0.03	93.6	0.05	92.5	0.07	61.2	0.084	45.3	77.42
630	0.014	91.1	0.04	82	0.07	55.6	0.09	42.5	0.12	35.2	61.28
760	0.02	77.1	0.06	68.1	0.1	48.1	0.14	36.1	0.17	27.2	51.32
1070	0.04	69.8	0.12	32.5	0.2	27	0.27	24.6	0.34	22.1	35.2
1690	0.1	42.1	0.31	20.8	0.5	18.8	0.68	17.4	0.86	15.8	22.98
2400	0.21	28.9	0.62	16.6	1	15.6	1.38	13.2	1.73	12.1	17.28
3500	0.45	19.5	1.32	15.5	2.15	12.8	2.94	10.5	3.68	9.9	13.64

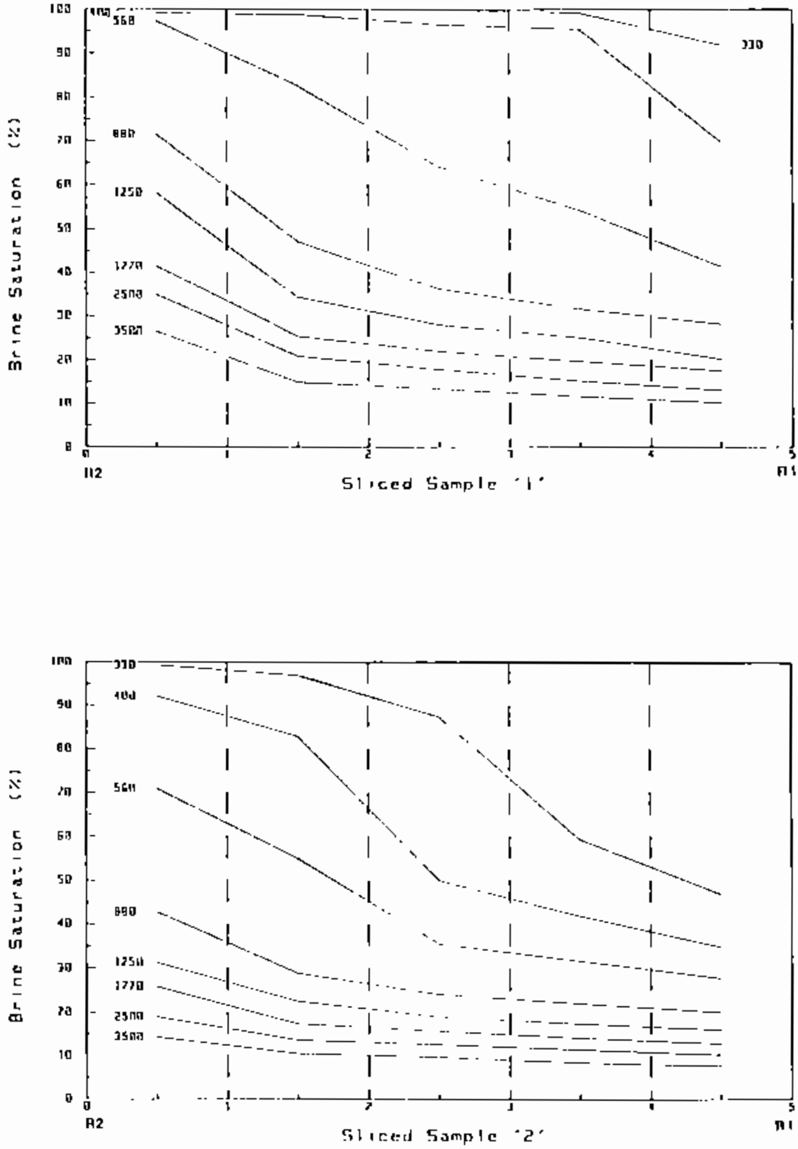

FIGURE 5 Brine saturation profile in air-brine drainage varying with centrifuge angular velocity.

TABLE 7 Experimental data using the new method.

AIR-BRINE DRAINAGE					
RPM	Pc Inlet/2 (kg/cm2)	BRINE SATURATION (%)			
		SAMPLE 1	SAMPLE 2	SAMPLE 3	SAMPLE 4
330	0.075	94.2	66.4	-	-
400	0.11	82.1	48.3	96.3	89.5
560	0.22	54.9	35	80.8	65.6
880	0.55	33.5	22.7	49.5	38.1
1250	1.11	25.1	17.8	36	31.6
1770	2.22	19.7	14.3	27.8	24.4
2500	4.43	15.7	11.5	19.7	19.1
3500	8.69	11.6	8.7	14.9	14.7

OIL-BRINE DRAINAGE			
RPM	Pc Inlet/2 (kg/cm2)	BRINE SATURATION (%)	
		SAMPLE 1	SAMPLE 2
530	0.054	93.7	66.1
630	0.075	78.7	48.7
760	0.11	65.7	39.5
1070	0.22	41.9	24.6
1690	0.5	27.7	17.5
2400	1.11	23.2	13.5
3500	2.36	18	11.5

it becomes considerable, but in this range brine saturation changes only a little being near the irreducible saturation point.

The exact capillary pressure curve is derived from the average brine saturation vs. the inlet capillary pressure using the two less approximated solutions: those of Rajan (A3) and Forbes (A4).

Rajan's equation requires a data fitting which is performed in this paper by a particular hyperbolic function (Glotin *et al.*, 1990; Ragazzini, 1991):

$$S(P_c) = \begin{cases} 100 & P_c \leq P_{threshold} \\ \dfrac{A}{P_c^{E}} + B & P_c > P_{threshold} \end{cases} \tag{2}$$

where the $P_{threshold}$ value is extrapolated setting the 100% brine saturation in the hyperbolic function.

The comparison among the experimental and calculated results of all the four samples is plotted in Figures 6-8.

It can be noted that although Forbes' curve is quite irregular it has nearly the same trend as Rajan's for all the samples studied.

As shown in Figures 6-8 the inlet piece capillary pressure curve of both the air-brine and oil-brine drainage is very close to their respective solutions calculated using (A4) and (A5).

Comparing the capillary pressure curves to the corresponding saturation profile, it is possible to deduce with a good approximation that the end- effect in the sample, which affects the saturation, is in the last centimeter for all the speeds used.

So using an end-piece 1 cm long, weighing the whole core samples to calculate their average saturation and considering the average capillary pressure in the whole system it has been possible to obtain the plot of the capillary pressure curve as shown in Figures 6-8.

The new technique gives good results having the same trend as the other curves. It has a good reproducibility and has the same accuracy within the experimental error which was computed (in previous studies) to be less than 3%.

CONCLUSIONS

1. The technique described gives the exact capillary pressure curve directly from centrifuge experimental data without mathematical elaborations and, for this reason, it can be considered the first successful experimental method to do this in literature.
2. It is proposed to equip the sample with a porous end-piece (1 cm long if the sample is 5 cm long) which is in capillary

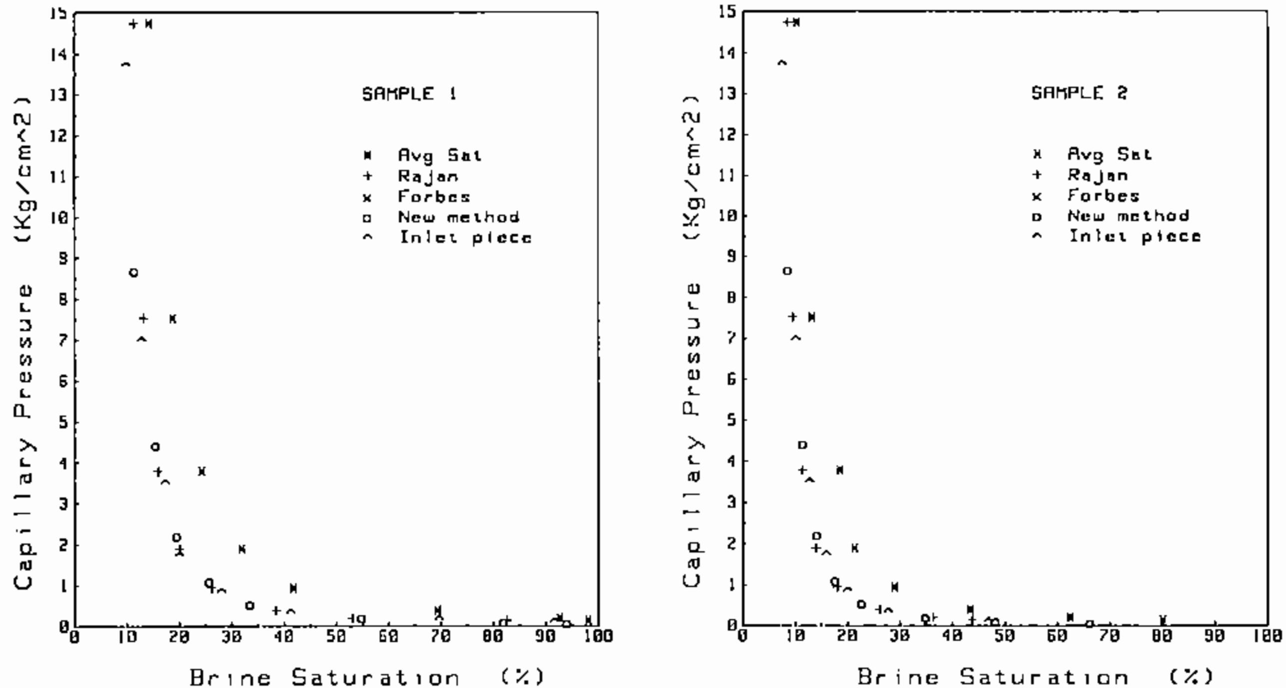

FIGURE 6 Air-brine capillary pressure curves comparison of the most permeable samples.

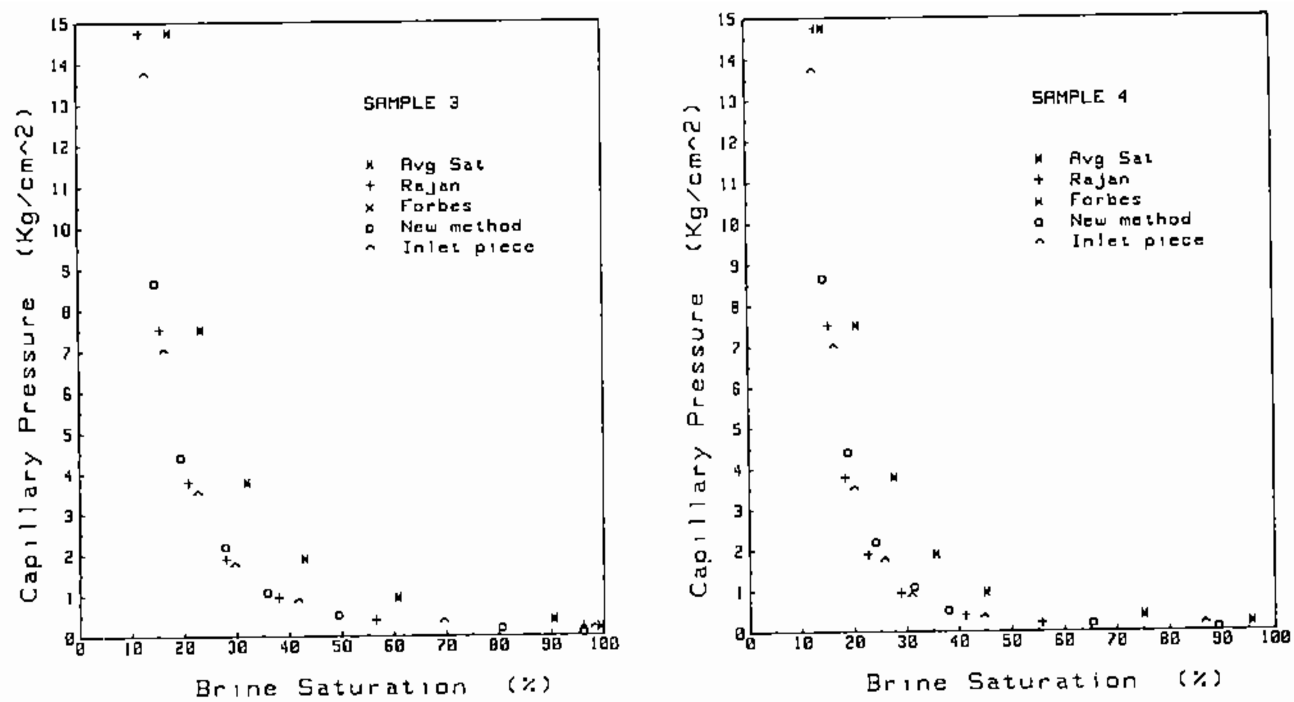

FIGURE 7 Air-brine capillary pressure curves comparison of the least permeable samples.

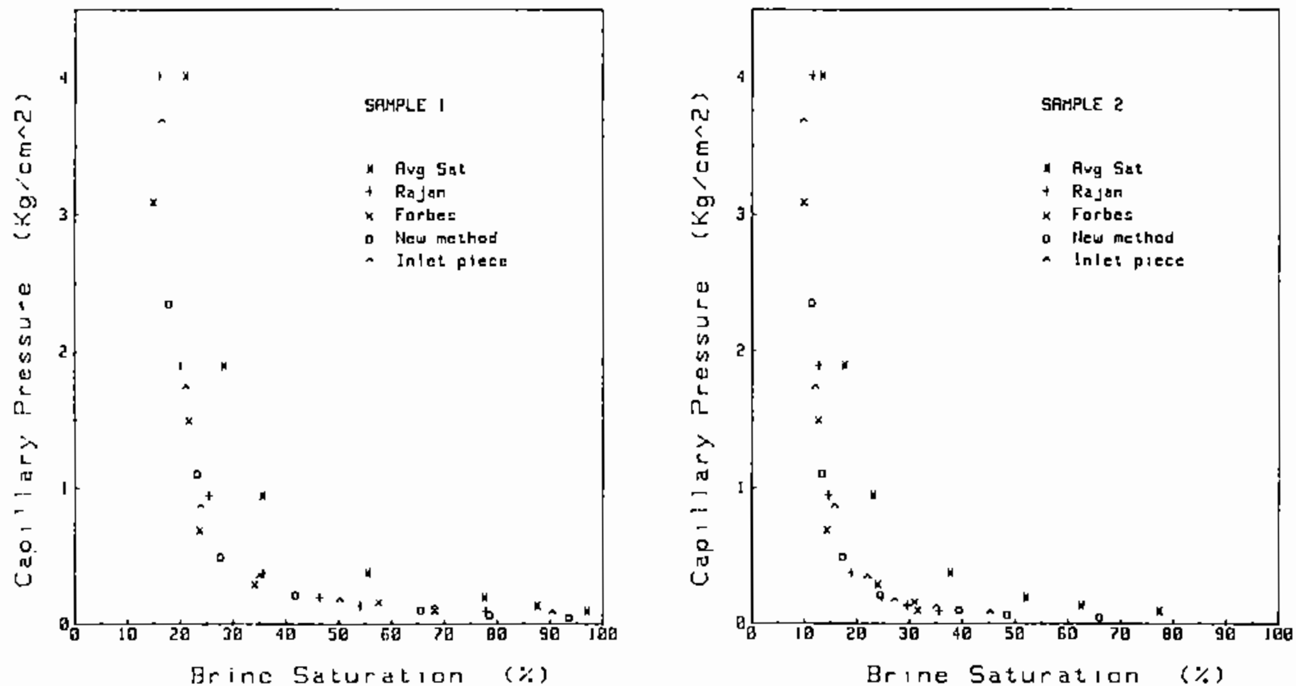

FIGURE 8 Oil-brine capillary pressure curves comparison of the most permeable samples.

contact with the sample. The curve is obtained from the saturation data (obtained by stopping centrifuge and weighing only the sample) vs. the average capillary pressure in the whole system (sample plus end-piece).

3. Its validation is demonstrated by the comparison to the solutions of Rajan and Forbes using homogeneous Sandstone samples having different permeabilities both in air-brine and oil-brine drainages and is supported by the saturation profile in the samples subdivided in five pieces kept in capillary contact with each other.

4. The proposed technique has the same accuracy within experimental error and is rapid because complex elaborations of the experimental data aren't necessary.

5. A study is being prepared to check the validity of the technique here proposed in the case of inhomogeneous cores of different lithologies.

NOMENCLATURE

A,B,E	fitting coefficients
D	sample diameter
K	sample permeability
L	sample length
P_c	capillary pressure at any point along the sample length
P_{c1}	capillary pressure at the inlet face of the sample
r	radial distance from the centrifuge rotation axis to a point in the sample
R_1	r at the inlet face of the sample
R_2	r at the outlet face of the sample
S	saturation
$\overline{S}$	average saturation
w	angular velocity
ϕ	sample porosity
$\Delta\varrho$	density difference between fluids

ACKNOWLEDGEMENTS

The authors would like to thank G.D.Fanti (DB Stratabit) for his valuable contribution, P.Forbes (IFP) for his useful suggestions and the management of AGIP SpA for the permission to publish this paper.

APPENDIX

The average saturation is related to the local saturation by the expression:

$$\overline{S} = \frac{1}{R_2 - R_1} \int_{R_1}^{R_2} S(r)\, dr \,. \tag{A1}$$

Substituting the variable r by P_c and calculating dr (from Equation 1) it follows that the average saturation is expressed by:

$$\overline{S}(P_{c1}) = \frac{1+R}{2\, P_{c1}} \int_{0}^{P_{c1}} \frac{S(P_c)\ \ dP_c}{\sqrt{1 - \frac{P_c}{P_{c1}}\,(1 - R^2)}} \tag{A2}$$

where $R = R_1/R_2$ and $P_c(R_2) = 0$.

The problem consists of inverting this Volterra integral equation of the first kind to obtain the local curve $S(P_c)$ from the experimental data $S(P_{c1})$.

Some studies to solve this equation are based on experimental data differentiation and some others require both differentiation and integration, all of them involving more or less pronounced approximations.

Hassler and Brunner (1941), neglecting the centrifugal gravity gradient, obtained a solution which is valid only in the case of very short samples (for $R > 0.7$). It underestimates the saturation values and the error involved is small only in the low saturation range.

Hoffman (1963) and later van Domselaar (1984), derived approximated solutions of Equation (A1). In particular van Domselaar's solution systematically overestimates the saturation values. It is accurate in the high saturation range for longer samples (Melrose, 1988).

However, these solutions, involving calculations of differences, are highly sensitive to experimental error.

Rajan (1986) derived the exact result and then, making use of an assumption about the slope of the average saturation, obtained the solution:

$$S(P_{c1}) = \overline{S}(P_{c1}) + \frac{2R}{1+R} P_{c1} \frac{d\overline{S}(P_{c1})}{dP_{c1}} + \frac{R}{(1-R^2)} \int_0^{P_{c1}} \left[\frac{1}{\left(1 - \frac{P_c}{P_{c1}}(1-R^2)\right)^{1/2}} - 1 \right]^2 \frac{d\overline{S}(P_c)}{dP_c} dP_c \qquad (A3)$$

which is valid over the range $0.5 \leq R \leq 1$. It is more accurate than the previous solutions here described and can be considered the best approximation currently available.

Due to the presence of derivatives and of an integral, this approach requires the use of a function fitting saturation experimental data vs. capillary pressure.

Many authors (Ruth and Wong 1988, 1990; Ayappa *et al.* 1989; Hermansen *et al.* 1991; Nordtvedt and Kollvelt, 1991) proposed different approaches to reduce the experimental data both in a given functional form provided by polynomial, exponential or hyperbolic functions or using modified midpoint procedure and "spline functions" that make "no a priori assumption of the form of the curve".

Forbes (1991) proposed two good solutions to study the capillary pressure curve. The first requires a curve fitting while the second, which he recommends, converts the raw experimental data requiring "no smoothing, fitting, averaging or forcing of data".

This last solution is derived from the observation that the real curve has to be between the Hassler-Brunner and van Domselaar solutions.

Referring the subscript $i-\mu$ $(0 \leq \mu \leq 1)$ to the value of the function at pressure $P_i - \mu[P_i - P_{i-1}]$,

$$S_{\alpha_{i-1/2}} = \frac{\overline{S}_i - (P_{i-1}/P_i)^{1+\alpha}\ \overline{S}_{i-1}}{1 - (P_{i-1}/P_i)^{1+\alpha}}$$

$$S_{\beta_i} = (P_{i-1}/P_i)^{1+\alpha} S_{\beta_{i-1}} + \frac{1-(P_{i-1}/P_i)^{1+\beta}}{1-P_{i-1}/P_i}\ \overline{S}_i - \frac{P_{i-1}}{P_i}\ \overline{S}_{i-1}$$

he obtained:

$$S_{i-1/2+B/4} = (1-B)\ S_{\alpha_{i-1/2}} + B/2\ S_{\beta_i} \qquad \text{(A4)}$$

where $B = 1-R^2$, $0 \leq B \leq 1$, $\alpha = \dfrac{R_2-R_1}{R_2+R_1}$, $\beta = 2/\alpha$

with the constraint $S_{j+1} \leq S_j$ that prevents possible oscillation of results.

The quite irregular shape of this solution seems to reproduce the raw experimental data trend better than the other solutions.

REFERENCES

AYAPPA, K.G., DAVIS, H.T., DAVIS, E.A., GORDON, J. (1989) Capillary pressure: centrifuge method revisited. *AIChE Journal* Vol. 35, n° 3, 365-372

FORBES, P. (1991) Simple and accurate method for converting centrifuge data into drainage and imbibition capillary pressure curves. *SCA Conference Paper* n° 9107

GLOTIN, G., GENET, J., KLEIN, P. (1990) Computation of drainage and imbibition capillary pressure curves from centrifuge experiments. *SPE Paper* n° 20502, 313-324

HASSLER, G.L., BRUNNER, E. (1945) Measurement of capillary pressures in small core samples. *Trans. AIME*, **160**, 114-123

HERMANSEN, H., ELIASSEN, O., GUO, Y., SKJAEVELAND, S. (1991) Capillary pressure - A new, direct method. *SCA Conference Paper*

HOFFMAN, R.N. (1963) A technique for the determination of capillary pressure curves using a constantly accelerated centrifuge. *SPEJ*, **3**, 227-235

MELROSE, J.C., (1988) Interpretation of centrifuge capillary pressure data. *The Log Analyst*, **1**, 40-47

NORDTVEDT, J.E., KOLLVELT, K. (1991) Capillary pressure curves from centrifuge data by use of spline functions. *SPERE*

OMOREGIE, Z.S. (1988) Factors affecting the equivalency of different capillary pressure measurement techniques. *SPEFE*

RAGAZZINI, G. (1991) Capillary measurements on Berea sandstone. *ENI Group internal report* (in Italian)

RAJAN, R.R. (1986) Theoretically correct analytical solution for calculating capillary pressure-saturation from centrifuge experiment. *SPWLA* J, 1-18

RUTH, D., WONG, S. (1988) Calculation of capillary pressure curves from data obtained by the centrifuge method. *SCA Conference Paper* n° 8802

RUTH,D., WONG, S. (1990) Centrifuge capillary pressure curves. *JCPT*, **3**, 67-72

VAN DOMSELAAR, H.R. (1984) An exact equation to calculate actual saturations from centrifuge capillary pressure measurement. *Rev. Tec. Intevep.*, Vol. 4, n° 1, 55-62